Nonequilibrium Thermodynamics of Turbulence-Driven Rotors

N. Francois,* H. Xia, H. Punzmann, and M. Shats
Research School of Physics, The Australian National University, Canberra ACT 2601, Australia

(Received 26 August 2019; revised manuscript received 16 March 2020; accepted 21 May 2020; published 24 June 2020)

We characterize a process of energy extraction via rectification of strongly turbulent flow by using tools of stochastic thermodynamics. We study the dynamics of an asymmetric autonomous rotor that shows biased direction of rotation when placed in a stream. We give experimental evidence that a fluctuation theorem can be used to describe the work injected in the rotor via its coupling with the turbulent flow structure. This approach allows to measure the mean power extracted from the chaotic fluid motion over a broad range of turbulent kinetic energy. A nontrivial dependence of the rotor power on flow kinetic energy is identified. This observation is described by a model taking into account the dissipation of the rotor energy and the temporal memory of coherent structures present in the turbulent flow.

DOI: 10.1103/PhysRevLett.124.254501

The conversion of the kinetic energy of a flow into useful work constitutes a central problem of fluid mechanics that can benefit many applications in the area of renewable energy, such as wave and wind energy, as well as in biology [1–7]. To operate efficiently, many energy converters rely on a steady flow component dominating the fluid dynamics (driven by a sustained wind or regular wave) [2,8]. However, natural flows present a substantial level of turbulence and therefore they fluctuate over a broad range of time and length scales. The impact of turbulence on the power harvested from the flow and on the energy loss by conversion systems remains an outstanding fundamental question [2,8–10]. The utilization of fluid kinetic energy is particularly difficult when turbulent fluctuations are acute on a timescale comparable to the response time of the converters. Another recurrent problem is related to the complex spatial structure of turbulent flows, in particular the presence of coherent structures that are either inherently present or generated in the wake of neighboring converters [9,11–18]. It is therefore important to devise model experiments to bring insights into these problems.

In this Letter, we experimentally study the power extracted by an autonomous rotor from a strongly turbulent flow [19]. These flows show no steady velocity component and include coherent structures. In this system, the key to the extraction of useful work is the efficient coupling of the rotor with the Lagrangian structure of the flow [19–21]. Important features of the process of energy extraction from this strongly out-of-equilibrium flow have not been explored yet. In particular, the torque acting on the rotor was not measured, and consequently the power extracted from the turbulent flow could not be characterized. Here, we take advantage of tools developed in stochastic thermodynamics to measure these quantities.

The framework of stochastic thermodynamics offers noninvasive tools to characterize the work generated by out-of-equilibrium systems in contact with an energy reservoir [22,23]. Seminal works have shown that theoretical relations, known as fluctuation theorems (FT), can be applied to study fluctuations in turbulent flows [24,25], liquid crystal electroconvection [26], mechanical waves [27], or ratchet effects in granular media [28,29]. Yet the use of FT to describe chaotic dynamics in macroscopic systems remains scarce, and therefore most of its potential applications remain to be explored. Here, we show that an FT can be applied to the work extracted by turbulence-driven rotors. The FT allows a noninvasive characterization of the rotor power that is shown to have a nontrivial dependence on the flow kinetic energy.

In these experiments, turbulent flows are produced at a liquid surface perturbed by parametrically excited Faraday waves. The waves are generated in a circular container (diameter = 290 mm) filled with water up to its brim (water depth = 85 mm). The container is vertically vibrated at a frequency of $f_s = 60$ Hz, and the acceleration takes values from 0.5 g to 1.2 g. Although energy is injected into the vertical oscillations of Faraday waves, part of this energy is converted into chaotic horizontal fluid motion via the generation and nonlinear interaction of horizontal vortices [30–35]. The size of these vortices determines the flow forcing scale, $L_f = 4.4$ mm at $f_s = 60$ Hz [36,37]. The wave-driven turbulent motion is random, with no mean flow component, and it shows Gaussian velocity fluctuations. The rms velocity U of these fluctuations depends on the kinetic energy accumulated over a broad range of scales by a process referred to as the inverse energy cascade in the context of 2D turbulence [30,31,36,38–40]. A characteristic time of the flow is the lifetime of its Lagrangian coherent structures given by $T_B \approx 30 \times L_f/U$, and it is in the range of $2\ \text{s} < T_B < 20\ \text{s}$. The rotor is made of thermoplastic (ABS) and printed on a 3D-printer. The density of the ABS matches that of water;

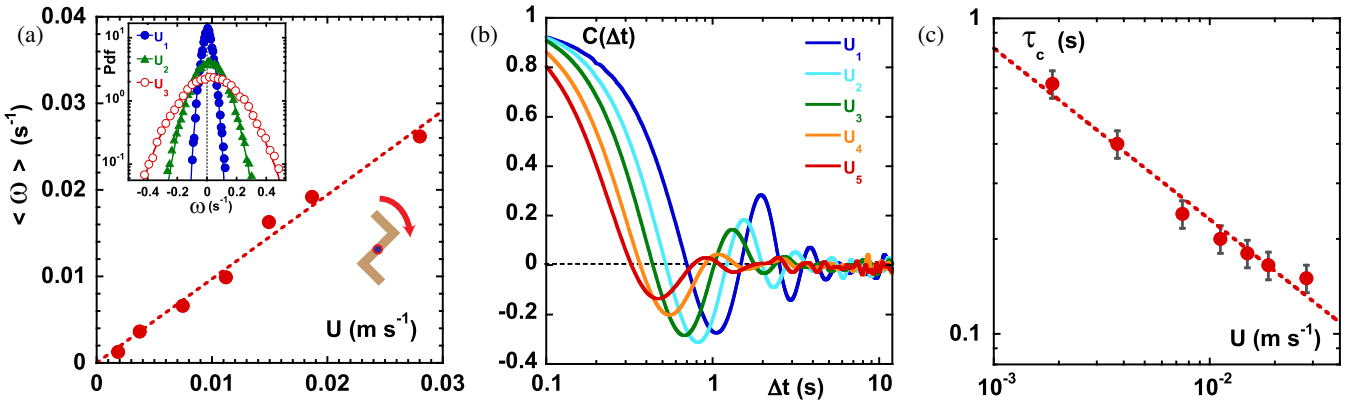

FIG. 1. (a) Mean angular velocity $\langle\omega\rangle$ of the rotor versus the flow rms velocity U. Inset: Probability distribution functions of the angular velocity ω measured at different rms flow velocities ($U_1 < U_2 < U_3$) in the range of $0.001 < U < 0.03$ m s^{-1}. In the lower right corner, a schematic of the rotor shows its geometry, its axis of rotation (blue dot), and its direction of rotation (red arrow). (b) Temporal autocorrelation functions $C(\Delta t) = \langle\delta\omega(\Delta t)\delta\omega(t_0)\rangle/\langle\delta\omega^2\rangle$ measured at different levels of turbulent intensity ($U_1 <, \ldots, < U_5$) in the range of $0.001 < U < 0.03$ m s^{-1}. (c) Integral timescale τ_c versus the flow rms velocity U. The dotted line indicates a $\tau_c \propto 1/\sqrt{U}$ scaling.

hence, the rotor is neutrally buoyant. The rotor is an asymmetric floating object made of two L-shaped arms [see schematics in Fig. 1(a)]. The rotor has a 50 mm wingspan, a 5 mm width, and a 0.4 mm thickness. Its lateral arms are 25 mm long. The rotors are printed with a 3-mm-diameter hole at the location of the axis of rotation; an externally fixed 0.5-mm-diameter needle serves as the pivot. In this configuration, there is almost no friction between the floating rotor and the pivot axis.

Due to its asymmetry, the rotation of the rotor is biased in one direction. As demonstrated in [19], this direction is determined by the force originating from the rectification of the flow inside the L-shaped arm. We study the dynamics of the angular velocity $\omega = \partial\theta/\partial t$ of the rotor as a function of the turbulent flow energy U^2. The angular position θ of the rotor is recorded by a camera at a frame rate of 105 fps during 20-minute-long experimental runs. Large data samples allows us to characterize with great accuracy the mean angular velocity $\langle\omega\rangle$ and the angular velocity fluctuations $\delta\omega = \omega - \langle\omega\rangle$, where $\langle\rangle$ denotes statistical averaging. The present analysis is performed on data collected after the system has reached a steady state when $\langle\omega\rangle$ is steady in time. Figure 1(a) shows that the mean angular velocity $\langle\omega\rangle$ is a linear function of the flow rms velocity U. The probability distribution function (PDF) of ω is plotted in the inset in Fig. 1(a). The PDF is well fitted by a Gaussian distribution with strong fluctuations around its mean and a variance $\langle\delta\omega^2\rangle$, which increases with the flow energy. In terms of energy conversion of a flow, rotors operate in an interesting regime; indeed, rotors extract energy from Lagrangian coherent structures whose characteristic size has to be smaller than the rotor span [19] and that have a characteristic lifetime much smaller than the rotor rotation period ($\langle\omega\rangle < 2\pi/T_B$, the dynamics of the rotor is much slower than that of the flow). The Reynolds number of the rotor is in the range (1–20). These seemingly intermediate values actually correspond to fully developed 2D turbulence [31,41–43].

To further characterize the rotor dynamics, we compute the temporal autocorrelation function $C(\Delta t)$ of the fluctuations $\delta\omega(t)$ as follows: $C(\Delta t) = \langle\delta\omega(\Delta t)\delta\omega(t_0)\rangle/\langle\delta\omega^2\rangle$, where $\Delta t = t - t_0$ is the time interval. As shown in Fig. 1(b), the autocorrelation function $C(\Delta t)$ is strongly dependent on the flow rms velocity U. It decays faster with the increase of U. Moreover, it exhibits strong oscillations that are dampened only after several seconds at low value of the flow energy. This behavior reflects both the importance of inertia in this system and a strong coupling of the rotor with the turbulent flow [19]. We also compute the integral time τ_c as $\tau_c = \int_0^\infty C(\Delta t)dt$. The timescale τ_c is a decreasing function of U [see Fig. 1(c)]. One can see that $\tau_c \propto 1/\sqrt{U}$.

The mean angular velocity $\langle\omega\rangle$ is constant in time. This suggests that the rectification phenomenon can be described by a constant torque P acting on the rotor. The work done by the torque over a time interval τ corresponds to the energy W_τ extracted from the turbulent flow by the rotor. It is given by $W_\tau(t) = \int_t^{t+\tau} P\omega(t)dt = P\Delta\theta$, where $\Delta\theta = \theta(t+\tau) - \theta(t)$ is the angular displacement over a time interval τ. To characterize the work, we need to measure the torque P. To achieve this, we test the existence of an FT for the fluctuations of $W_\tau(t)$ [23] by looking for a relation in the following form:

$$S = \ln\left[\frac{H(W_\tau)}{H(-W_\tau)}\right] = \ln\left[\frac{H(\Delta\theta)}{H(-\Delta\theta)}\right] = \beta\Delta\theta, \qquad \tau > \tau_c, \tag{1}$$

where $H(W_\tau)$ is the PDF of W_τ. Most importantly, the measurement of β will allow us to determine the torque P.

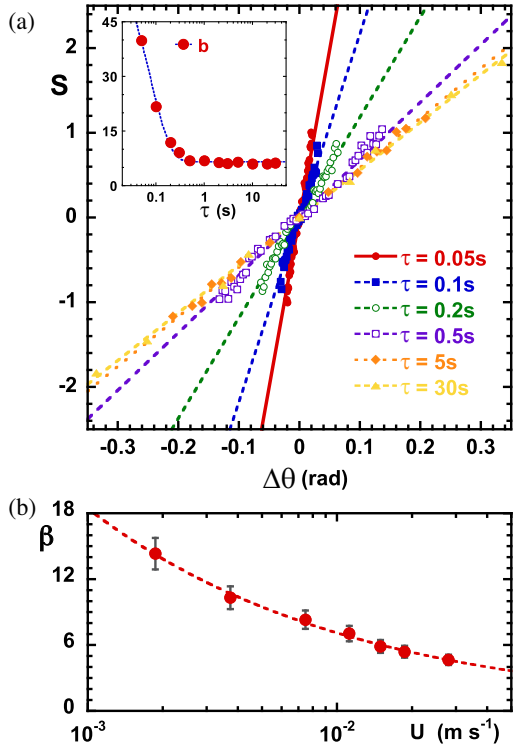

FIG. 2. (a) Functions $S(\Delta\theta)$ versus angular displacement $\Delta\theta$ for increasing values of the time interval τ (at fixed flow rms velocity $U = 0.015$ m s^{-1}). Inset: Slope b [defined as $S(\Delta\theta, \tau) = b\Delta\theta$] as a function of τ. (b) Parameter β versus the flow rms velocity U. The dotted line indicates a $\beta \propto 1/\sqrt{U}$ scaling.

Figure 2(a) shows the behavior of S as a function of $\Delta\theta$ for different values of τ. The function S increases linearly with $\Delta\theta$ for all values of τ, i.e., $S(\Delta\theta) = b(\tau)\Delta\theta$. For values of τ larger than τ_c, the functions S collapse onto a single line. This collapse is characterized in the inset of Fig. 2(a) by measuring how the slope b of S depends on τ: b decreases with τ until it plateaus at a value β for $\tau > \tau_c$. The dependence of the parameter β on the turbulent flow energy has been tested over a broad range of turbulence intensities. Figure 2(b) shows that β decreases with the increase of the flow velocity U. The behavior can be fitted by $\beta \propto 1/\sqrt{U}$.

Analogies with experiments performed on microscopic rotating systems [23] suggest that β should be related to the torque P via the relation $\beta = P/E_r$, where E_r is a characteristic energy that plays the role of an effective temperature. In the case of microscopic rotors, E_r is the temperature of the thermal bath $E_r = k_B T$ [23]. In our macroscopic system, fluctuations are produced by the turbulent dynamics and not by thermal noise. In this highly nonequilibrium context, a challenging problem lies in determining the energy scale E_r [22]. A possible choice for E_r is the energy of the angular velocity fluctuations $J\langle\delta\omega^2\rangle$, where J is the moment of inertia of the rotor.

The energy of angular velocity fluctuations is linearly proportional to the turbulent flow energy $E_r \propto U^2$ as seen in Fig. 3(a). This indicates that the flow kinetic energy can be used as the characteristic energy scale in the FT. Figure 3(a) shows the value of the torque derived from $P = \beta \times E_r$. Note that P strongly depends on the flow rms velocity and that it follows a scaling $P \propto U^{1.5}$.

Wave-driven turbulent flows are fueled by the vorticity generated by the waves at the fluid surface [30,44]. It has recently been reported that turbulence does not invade the entire fluid bulk but remains localized in a 2-mm-thick layer near the fluid surface [45]. While the previous results concern the dynamics of *thin* rotors whose thickness is 0.4 mm, we now investigate the behavior of a 2-mm-thick rotor that will strongly interact with the turbulent boundary layer. The mean angular velocity $\langle\omega\rangle$ of thick rotors is proportional to the flow velocity U. The function S of thick rotors is linear in $\Delta\theta$, and it collapses on a unique curve for

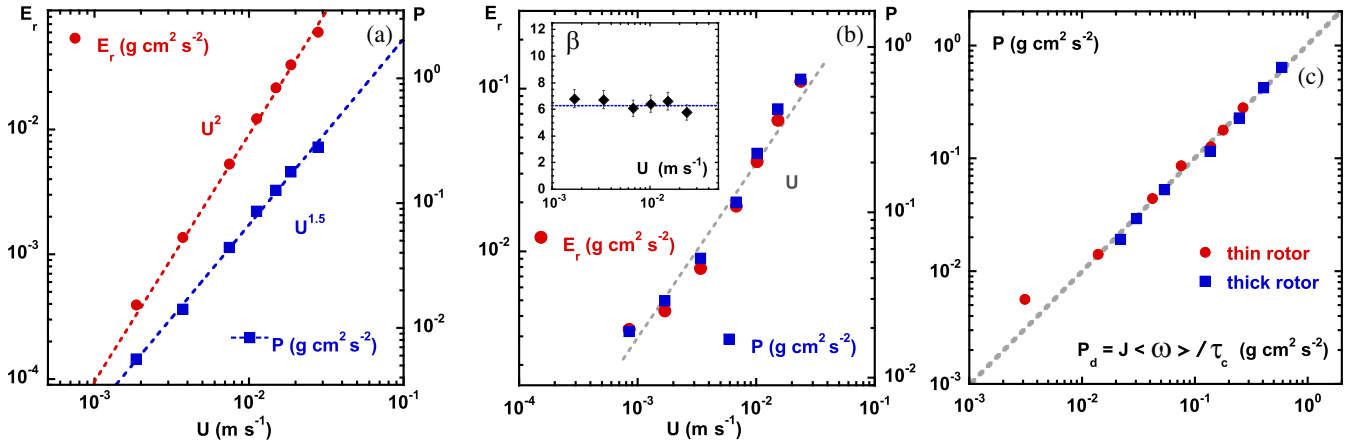

FIG. 3. (a) Energy $E_r = J\langle\delta\omega^2\rangle$ of angular velocity fluctuations and torque P acting on the thin rotor versus flow rms velocity U. The torque is derived from the relation $P = \beta \times E_r$. (b) Energy E_r and torque P measured for a thick rotor as functions of U. Inset: Parameter β, measured for a thick rotor, versus U. (c) Torque $P = \beta \times E_r$ as a function of the model $P_d = J\langle\omega\rangle/\tau_c$.

large values of τ. This allows us to measure the parameter β, which is constant over a range of the rms flow velocities [see inset of Fig. 3(b)]. The change of thickness of the rotor also affects the energy of angular velocity fluctuations. As shown in Fig. 3(b), the dependence of E_r on the turbulent flow energy is modified, and we observe $E_r \propto U$. These two results have an impact on the measurement of the torque via the relation $P = \beta \times E_r$. Figure 3(b) shows that $P \propto U$ for thick rotors. The energy extraction process depends on the rotor thickness.

To gain further insights into this effect, we now compare the torque P measured via the FT with the value predicted by a simple model. In the latter, the torque P is balanced by a linear drag $P_d = C_d\langle\omega\rangle$, where C_d is the drag coefficient. The dissipation in our system can be characterized by the integral time τ_c derived from the autocorrelation function of $\delta\omega$. Indeed, the drag coefficient can be estimated as $C_d = J/\tau_c$. In contrast to the thin rotor, the timescale τ_c of a thick rotor is independent of the flow energy, and $\tau_c = 0.25$ s. This impacts the drag coefficient, which is a function of the flow energy $C_d \propto \sqrt{U}$ for a thin rotor while it is a constant for a thick rotor. Figure 3(c) confirms that the measurement of the torque P is equal to the estimate of P_d. This is observed for both the thin and thick rotors over a broad range of turbulent flow energies. This suggests that the dependence of the torque P on the rotor thickness [see Figs. 3(a) and 3(b)] is related to the drag coefficient C_d, i.e., to differences in the dissipation of the rotor energy.

We can now measure the work and the power extracted by the rotors from wave-driven turbulence. The inset of Fig. 4 shows a typical dynamics of the work $W_{10\tau_c}(t)$ produced by a thin rotor over time intervals of $10\tau_c$. The work fluctuates strongly with time around a negative mean value (negative values correspond to extracted energy).

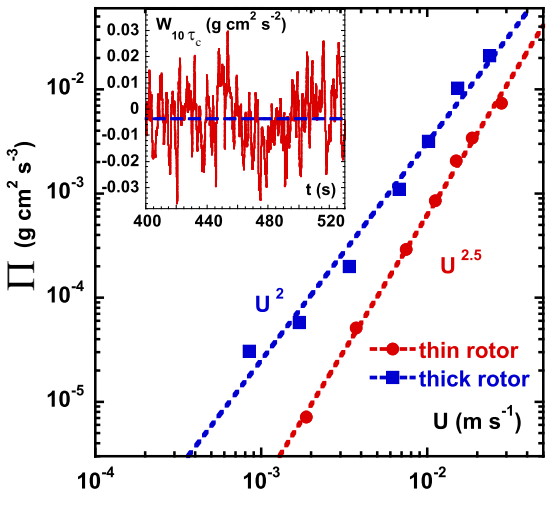

FIG. 4. Mean power Π extracted from turbulence by thin and thick rotors. Inset: Dynamics of the work $W_{10\tau_c}(t)$ extracted by a thin rotor over time intervals of $10\tau_c$ at $U^2 = 2.2 \times 10^{-4}\ m^2\ s^{-2}$. The blue dashed line indicates the average value $\langle W_{10\tau_c}\rangle$

Quantitatively, the rms value of the fluctuations is four times larger than the mean value. The mean power Π is estimated as $\Pi = P \times \langle\omega\rangle$ or similarly $\Pi = C_d \times \langle\omega\rangle^2$. Figure 4 shows that Π depends strongly on the turbulent flow energy. Although thicker rotors extract larger power than thin rotors, the scaling exponent of Π with the flow velocity U is larger for a thin rotor $\Pi \sim U^{2.5}$ (while $\Pi \sim U^2$ for thick rotors). Since $\langle\omega\rangle \propto U$ for both rotors, this difference in scaling is related to the dependence of the drag coefficient C_d on the rotor thickness. In [45], it is shown that the structure of the turbulent boundary layer below the surface is substantially different from that of the flow at the fluid surface, that is, only large and slow turbulent eddies persist in the fluid even few millimeters below the surface. The interaction of the rotor with this depth-dependent flow structure is clearly not trivial and deserves further characterization as a function of the rotor thickness t and boundary layer thickness L_b. The results presented here suggest that the ratio t/L_b mostly affects the dissipation process (i.e., C_d), while the propulsion velocity (i.e., $\langle\omega\rangle$) seems independent of it. To further characterize the energy extraction, we performed additional experiments in which an optical fiber cantilever was connected to one of the rotor arms. As it deforms, this cantilever exerts an elastic force on the rotor [46,47]. We found that a large amount of the rotational energy of the rotor can be directly converted into useful work; in this case the elastic energy stored in fiber deformations.

The two scaling laws for Π are different from the classic relation $\Pi \propto u^3$ used for the power generated by a turbine placed in a steady stream flowing at constant speed u. The origin of this difference lies in the operational principle of autonomous rotors. The key ingredient of the rectification phenomenon is the coupling of the rotor to riverlike coherent structures present in wave-driven turbulence [19]. In a nutshell, the corner of the rotor acts as a stagnation point for the flow, which forces a river to bend, thus creating a reaction force acting on the rotor's corner. The rivers have a finite lifetime T_B that is a function of the flow rms velocity $T_B \sim 1/U$ [21]. On the basis of the phenomenology introduced in [19], the rotor power can be described as $\Pi = \rho K U(U^2/L_f) f(T_B, \tau_c)$, where ρ is the fluid density, K is a geometric factor, and U^2/L_f is the centripetal acceleration characterizing the bending of rivers in the rotor's corner. The function $f(T_B, \tau_c)$ is the coupling factor between the flow fabric and the rotor. The coupling factor has to reflect both the river's lifetime T_B and the dissipation of the rotor energy via the timescale τ_c. The simplest choice is $f = T_B/\tau_c$, and the dependence of Π on the flow velocity is given by $\Pi \sim U^3 \times T_B/\tau_c$. The model predicts $\Pi \sim U^{2.5}$ for thin rotors and $\Pi \sim U^2$ in the case of thick rotors in agreement with our measurements.

In conclusion, a fluctuation theorem can be used to characterize the work extracted by turbulence-driven rotors. The experimental results highlight that the process of

energy extraction via rectification of turbulent fluid motion relies on both the dissipation of the rotor energy and on the characteristic lifetime of coherent flow structures.

This work was supported by the Australian Research Council Discovery Projects and Linkage Projects funding scheme (DP160100863, DP190100406, and LP160100477). N. F. acknowledges support by the Australian Research Council's DECRA Grant No. (DE160100742). H. X. acknowledges support from the Australian Research Council Future Fellowship (FT140100067).

*Corresponding author.
nicolas.francois@anu.edu.au

[1] E. Guyon, J.-P. Hulin, L. Petit, and C. D. Mitescu, *Physical Hydrodynamics* (Oxford University Press, New York, 2010).
[2] D. J. C. MacKay, *Sustainable Energy - Without the Hot Air* (UIT Cambridge Ltd, Cambridge, England, 2009).
[3] U. Lacis, N. Brosse, F. Ingremeau, A. Mazzino, F. Lundell, H. Kellay, and S. Bagheri, Nat. Commun. **5**, 5310 (2014).
[4] M. Shelley and J. Zhang, Annu. Rev. Fluid Mech. **43**, 449 (2011).
[5] C. Nov-Josserand, F. C. Hebrero, L. Petit, W. Megill, R. G. Diana, and B. Thiria, Bioinspiration Biomimetics **13**, 036006 (2018).
[6] D. N. Beal, F. S. Hover, M. S. Triantafyllou, J. C. Liao, and G. V. Lauder, J. Fluid Mech. **549**, 385 (2006).
[7] F. E. Fish and G. V. Lauder, Annu. Rev. Fluid Mech. **38**, 193 (2006).
[8] A. F. O. Falcao, Renewable Sustainable Energy Rev. **14**, 899 (2010).
[9] M. M. Bandi, Phys. Rev. Lett. **118**, 028301 (2017).
[10] J. Apt, J. Power Sources **169**, 369 (2007).
[11] J. J. Allen and A. J. Smits, J. Fluids Struct. **15**, 629 (2001).
[12] G. V. Iungo, F. Viola, S. Camarri, F. Port-Agel, and F. Gallaire, J. Fluid Mech. **737**, 499 (2013).
[13] A. K. M. F. Hussain, Phys. Fluids **26**, 2816 (1983).
[14] T. Peacock and G. Haller, Phys. Today **66**, No. 2, 41 (2013).
[15] H. D. Akaydin, N. Elvin, and Y. Andreopoulos, J. Intell. Mater. Syst. Struct. **21**, 1263 (2010).
[16] J. D. Hobeck and D. J. Inman, Smart Mater. Struct. **21**, 105024 (2012).
[17] N. Tobin and L. P. Chamorro, J. Fluid Mech. **855**, 1116 (2018).
[18] E. E. Bachynski and L. Eliassen, Wind Energy **22**, 219 (2018).
[19] N. Francois, H. Xia, H. Punzmann, and M. Shats, Phys. Rev. Fluids **3**, 124602 (2018).
[20] H. Xia, N. Francois, H. Punzmann, and M. Shats, J. Fluid Mech. **865**, 811 (2019).
[21] H. Xia, N. Francois, B. Faber, H. Punzmann, and M. Shats, Phys. Fluids **31**, 025111 (2019).
[22] S. Ciliberto, Phys. Rev. X **7**, 021051 (2017).
[23] S. Ciliberto, S. Joubaud, and A. Petrosian, J. Stat. Mech. (2010) P12003.
[24] S. Ciliberto, N. Garnier, S. Hernandez, C. Lacpatia, J.-F. Pinton, and G. Ruiz Chavarria, Physica (Amsterdam) **340A**, 240 (2004).
[25] M. M. Bandi, J. R. Cressman, and W. I. Goldburg, J. Stat. Phys. **130**, 27 (2008).
[26] W. I. Goldburg, Y. Y. Goldschmidt, and H. Kellay, Phys. Rev. Lett. **87**, 245502 (2001).
[27] O. Cadot, A. Boudaoud, and C. Touz, Eur. Phys. J. B **66**, 399 (2008).
[28] S. Joubaud, D. Lohse, and D. van der Meer, Phys. Rev. Lett. **108**, 210604 (2012).
[29] N. Kumar, S. Ramaswamy, and A. K. Sood, Phys. Rev. Lett. **106**, 118001 (2011).
[30] N. Francois, H. Xia, H. Punzmann, S. Ramsden, and M. Shats, Phys. Rev. X **4**, 021021 (2014).
[31] H. Xia and N. Francois, Phys. Fluids **29**, 111107 (2017).
[32] N. Francois, H. Xia, H. Punzmann, and M. Shats, Eur. Phys. J. E **38**, 106 (2015).
[33] S. V. Filatov, V. M. Parfenyev, S. S. Vergeles, M. Yu. Brazhnikov, A. A. Levchenko, and V. V. Lebedev, Phys. Rev. Lett. **116**, 054501 (2016).
[34] A. A. Levchenko, L. P. Mezhov-Deglin, and A. A. Pel'menev, JETP Lett. **106**, 252 (2017).
[35] N. Francois, H. Xia, H. Punzmann, F. W. Fontana, and M. Shats, Nat. Commun. **8**, 14325 (2017).
[36] N. Francois, H. Xia, H. Punzmann, and M. Shats, Phys. Rev. Lett. **110**, 194501 (2013).
[37] H. Xia, N. Francois, H. Punzmann, and M. Shats, Nat. Commun. **4**, 2013 (2013).
[38] R. Kraichnan, Phys. Fluids **10**, 1417 (1967).
[39] A. von Kameke, F. Huhn, G. Fernandez-Garcia, A. P. Munuzuri, and V. Perez-Munuzuri, Phys. Rev. Lett. **107**, 074502 (2011).
[40] A. Alexakis and L. Biferale, Phys. Rep. **767–769**, 1 (2018).
[41] G. Boffetta and R. E. Ecke, Annu. Rev. Fluid Mech. **44**, 427 (2012).
[42] G. Kokot, S. Das, R. G. Winkler, G. Gompper, I. S. Aranson, and A. Snezhko, Proc. Natl. Acad. Sci. U.S.A. **114**, 12870 (2017).
[43] N. Francois, H. Xia, H. Punzmann, and M. Shats, Sci. Rep. **5**, 18564 (2016).
[44] N. Francois, H. Xia, H. Punzmann, T. Combriat, and M. Shats, Phys. Rev. E **92**, 023027 (2015).
[45] R. Colombi, M. Schluter, and A. von Kameke, arXiv: 1911.11208. The thickness of the boundary layer is defined as the depth for which the rms turbulent horizontal velocity is halved.
[46] N. Francois, D. Lasne, Y. Amarouchene, B. Lounis, and H. Kellay, Phys. Rev. Lett. **100**, 018302 (2008).
[47] J. Yang, M. Davoodianidalik, H. Xia, H. Punzmann, M. Shats, and N. Francois, Phys. Rev. Fluids **4**, 104608 (2019).